THE JOURNAL OF PHYSICAL CHEMISTRY A

ARTICLE

pubs.acs.org/JPCA

Relation between Two-Photon Absorption and Dipolar Properties in a Series of Fluorenyl-Based Chromophores with Electron Donating or Electron Withdrawing Substituents

Aleksander Rebane,[*,†,‡] Mikhail Drobizhev,[†] Nikolay S. Makarov,[†,§] Erich Beuerman,[†] Joy E. Haley[∥] Douglas, M. Krein,[∥,⊥] Aaron R. Burke,[∥,⊥] Jonathan L. Flikkema,[∥,#] and Thomas M. Cooper[*,∥]

[†]Physics Department, Montana State University, Bozeman, Montana 59717, United States

[‡]National Institute of Chemical Physics and Biophysics, Tallinn, 12618 Estonia

[∥]Materials and Manufacturing Directorate, Air Force Research Laboratory, Wright Patterson Air Force Base, Ohio 45433, United States

[⊥]General Dynamics Information Technology, Dayton, Ohio 45431, United States

[#]SOCHE Student Research Program, Dayton, Ohio 45420, United States

Supporting Information

ABSTRACT: We investigate two-photon absorption (2PA) in a series of fluorenyl-based 9,9-diethyl-2-ethynyl-7-((4-R-phenyl)ethynyl)-9,9a-dihydro-4a*H*-fluorene chromophores with R being various electron donating (ED) and electron withdrawing (EW) groups. We use wavelength-tunable femtosecond laser pulses to measure the 2PA cross sections in the lowest dipole-allowed transition and show that the substituents with stronger ED or EW character enhance the peak 2PA cross section (up to $\sigma_2 \sim 60-80$ GM) while the neutral substituents lead to smaller cross sections, $\sigma_2 < 10$ GM. We apply two-level approximation to establish a quantitative relation between the 2PA in the pure electronic transition (0−0) and the corresponding change of the permanent electric dipole moment upon the excitation ($\Delta\mu$). This relation is elucidated by comparing $\Delta\mu$ values obtained from the 2PA measurements with quantum-chemical calculations and with measurements of solvatochromic shifts in a series of solvents. We show that the calculated $\Delta\mu$ correlate well with the values obtained from the 2PA spectroscopy. The $\Delta\mu$ values obtained from the solvatochromic shifts agree well with the above two methods for the chromophores with neutral or weak EW or ED substituents. On the other hand, stronger EW or ED end groups give much larger Stokes shifts, which lead to an overestimation of the $\Delta\mu$ values. We tentatively attribute this effect to the excitation-induced electronic density change occurring predominantly at the substituent side of the molecule, which causes the effective point dipole associated with the $\Delta\mu$ to interact more strongly with the surrounding solvent.

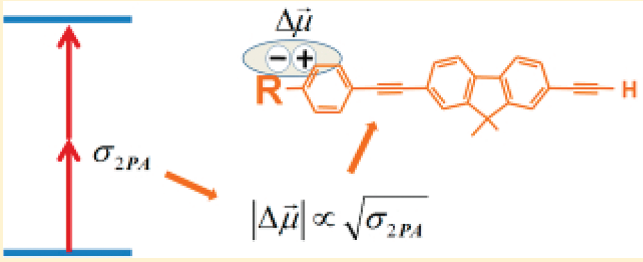

1. INTRODUCTION

Two-photon absorption (2PA) is an instantaneous nonlinear process, in which a chromophore absorbs two photons simultaneously.[1] A distinctive feature of the 2PA is that the rate of the absorption increases as the square of the incident photon flux. This property finds practical uses in fluorescence microscopy,[2] optical data storage,[3] intensity-dependent control of light transmission,[4] microfabrication,[5] and photodynamic therapy.[6]

Because the peak values of the 2PA cross sections of most off-the-shelf organic molecules in the visible- and near-IR range of wavelengths are rather small, $\sigma_2 \sim 1-10^2$ GM (1 GM = 10^{-50} cm^4 s photon^{-1}), it is important to design new chromophores with increased efficiency of the 2PA. Furthermore, as described in recent reviews,[7−10] such chromophores need to be optimized for particular applications and for particular ranges of wavelengths. Elementary quantum-mechanical perturbation theory considerations imply that the enhancement of the σ_2 may be achieved in two alternative, even though complementary, manners. The first would be to increase the value of the electronic transition dipole moments between the ground state (g) and intermediate excited states (i), as well as between the states (i) and the final excited state (f).[11] This property has been found, for example, in symmetrical ED−π−EW−π−ED or EW−π−ED−π−EW structural motifs, where −π− is a π-conjugated bridge or linker group.[12] In addition, when the excitation wavelength approaches the resonance wavelength of the intermediate g → i transition, then the resonance enhancement effect may further boost the σ_2 value, albeit in a limited range of wavelengths.[13] The second approach is based on the notion that larger 2PA efficiency may be expected if the system

Received: January 5, 2011
Revised: March 3, 2011

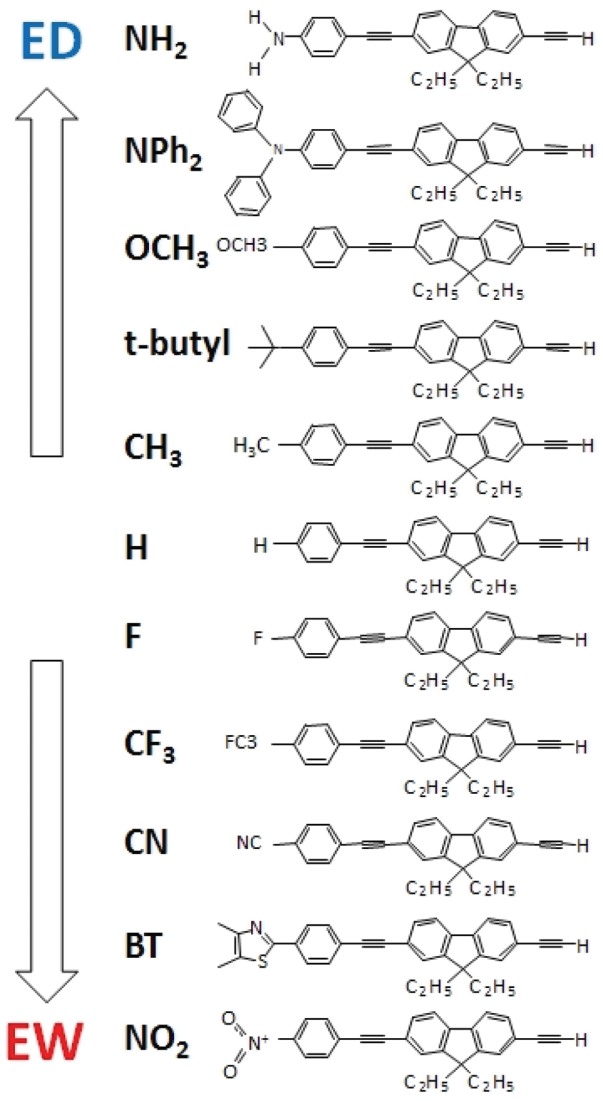

Figure 1. Chemical structures of the chromophores studied. The substituents X are listed in the order from neutral toward stronger ED or EW property.

possesses large transition dipole moment g → f as well as large difference between the permanent electric dipole moments in the g and f states.[14] Our recent studies of different organic dye molecules including substituted (diphenylamino)stilbenes, push−pull porphyrins, and carbazol-substituted stilbenes have shown that the 2PA cross section in the lowest-energy dipole-allowed purely electronic transition can indeed be quantitatively described by this so-called two-level model.[15] This method accounts for the change of the permanent dipole moment, $\Delta\mu$, in the same transition and has been instrumental for quantitative description of the 2PA with an appreciable absolute accuracy.[16] Moreover, this approach has facilitated determining the value of $\Delta\mu$ in a series of fluorescent proteins, and on this basis explaining the variation of the color hues in certain mutants.[17] The focus of this paper is to further investigate the quantitative relation between the dipolar properties of the chromophores and the 2PA.

Recently there has been an interest in the 2PA properties of bis(phenylethynyl)bis(tributylphosphine)platinum(II) complexes featuring fluorenyl-based ligands that are bound on both sides of the central platinum atom.[18] Attaching ligands with different ED groups and EW groups such as benzothiazolylfluorene, (diphenylamino)fluorene, and (dihexylamino)phenyl maintains the property of the heavy metal to channel the energy into a long-lived triplet state, while at the same time may also enhance the 2PA cross section.[18] It was reported that 2PA cross section of Pt-complexes may exceed that of the sum of the attached chromophores.[18] This so-called cooperative enhancement effect has been observed earlier in dendrimers,[19] but its role in the Pt complexes is still poorly understood. The current paper aims at elucidating how different ED- and EW groups influence the 2PA properties of the chromophores because this information may allow us to optimize the 2PA in the corresponding Pt-complexes.[20] We study a series of 11 fluorenyl-based chromophores end-capped with varying ED and EW groups. The structures are shown in Figure 1. The compounds are named in boldface by their substituent. Linear absorption- and emission properties within both the singlet- and triplet manifolds of the Pt complexes incorporating these ligands were reported in ref 20. Here we use wavelength-tunable femtosecond laser pulses to measure the 2PA spectra and cross section of the metal-free analogs of these chromophores with the goal of finding out how the different end groups change the 2PA properties especially in the lowest-energy dipole-allowed transition. We then use the 2PA cross section data to determine the change of the permanent electric dipole moment in the 0−0 component of the $S_0 \rightarrow S_1$ transition and show that these values correlate well with the calculations by quantum-chemical methods. To afford an independent check on these results, we use the solvatochromic shift technique to determine the $\Delta\mu$ and find that the solvatochromic data generally agrees with the other two methods. However, we also observe that chromophores with the strongest EW or ED end groups tend to give larger than expected solvatochromic shifts, which may be explained if we assume that the effective molecular point dipole is shifted off the center toward the substituted end of the molecule.

2. EXPERIMENTAL METHODS

Synthesis of the ligand series was described previously in ref 20. The UV−vis absorption spectra were measured in a 1 cm quartz cuvette using a Lambda 900 (Perkin-Elmer) spectrophotometer. Corrected steady state emission spectra were measured using a LS 50B (Perkin-Elmer) spectrofluorometer. The fluorescence anisotropy measurements were performed with the same instrument according to the standard procedure in L-configuration.[21] The viscosity was varied between the value of castor oil (10.17 $cm^2\ s^{-1}$) and that of chloroform (0.58×10^{-2} $cm^2\ s^{-1}$) by mixing the two solvents in the volume proportions: 1:0, 2:1, 3:2, 2:3, 1:4, and 0:1.[22] Fluorescence quantum yield (Φ_{fl}) was determined using relative actinometry as previously described.[23] Quinine sulfate was used as an actinometer with a known fluorescence quantum yield of 0.55 in 1.0 N H_2SO_4. Solvatochromic measurements were performed following the methodology described in ref 15. Briefly, fluorescence Stokes shifts were measured in solvents with different dielectric constant: octane (ε = 1.95), benzene (ε = 2.28), toluene (ε = 2.38), dibutyl ether (ε = 3.08), isobutyl isobutyrate (ε = 4.39), chloroform (ε = 4.81), isobutyl acetate (ε = 5.07), tetrahydrofuran (ε = 7.52), dichloromethane (ε = 8.93), and 4-methyl-2-pentanone (ε = 13.116). In these measurements the samples were placed in

dx.doi.org/10.1021/jp200129h |J. Phys. Chem. A XXXX, XXX, 000–000

1 cm cuvettes, and the dye concentration was adjusted such that the optical density at the excitation wavelength did not exceed OD < 0.1. The 2PA measurements described below were performed with higher concentrations and correspondingly higher peak optical densities, OD ~ 1.0.

Fluorescence lifetimes were measured using a C5680-21 synchro-scan streak camera (Hamamatsu) with 2 ps resolution. The fluorescence was excited using frequency-doubled output of a mode-locked Ti:sapphire femtosecond oscillator (Coherent Mira 900) pumped by a continuous wave (CW) frequency-doubled Nd:YVO_4 laser (Coherent Verdi 5).

The 2PA measurements were performed in toluene solutions and using fluorescence technique described in detail earlier.[24] A Ti:sapphire femtosecond oscillator seeded a 1 kHz repetition rate Ti:sapphire femtosecond regenerative amplifier (Legend HP, Coherent). The pulses from the amplifier were frequency-converted with a TOPAS-C femtosecond optical parametric amplifier (Light Conversion). The OPA signal beam wavelength was continuously tunable from λ_{ex} = 1100 to 1600 nm (λ_{ex} = 550−800 nm after second harmonic generation); the idler beam wavelength was λ_{ex} = 1600−2200 nm (λ_{ex} = 800−1100 nm after SHG). The OPA output pulse energy was 100−200 μJ (SHG pulse energy was 20−30 and 5−10 μJ for signal and idler, respectively).

The sample solution in a 1 cm spectroscopic cuvette was placed ~15 cm behind a f = 25 cm focusing lens. A small fraction of the excitation beam was split off by a glass plate and was directed to a pyroelectric detector (J3-02, Molectron) used for reference. The maximum pulse energy at the sample was about 1−10 μJ. The fluorescence was collected at right angle with respect to the excitation beam with a spherical mirror (f = 50 cm, diameter d = 10 cm) and focused with a unity magnification ratio on the entrance slit of an imaging diffraction grating spectrometer (Triax 550, Jobin Yvon). Sample absorbance spectrum was checked for possible photochemical damage before and after the 2PA measurement but no such changes were observed. The raw 2PA spectrum (in relative units) was obtained by measuring the intensity of the two-photon excited fluorescence as a function of the OPA wavelength, where the fluorescence intensity was normalized to the square of the reference channel intensity. The quadratic dependence of the 2PA on the excitation intensity was checked to exclude possible artifacts, e.g., due to linear absorption. The measured relative spectra were then corrected with respect to the previously characterized 2PA standards.[24] Absolute 2PA cross sections were determined for each OPA wavelength range by the relative fluorescence technique using the 2PA reference standards.[24]

Calculations were done using Gaussian 09W, Version 7.0.[25] The chromophores were modeled as 2-ethynyl-7-((4-X-phenyl)ethynyl)-9,9a-dihydro-4a*H*-fluorene in a vacuum. We performed DFT energy minimizations for the ground state using B3LYP/6-31 g(d). TDDFT calculations were done using CAM-B3LYP/6-31+G(d). The split-valence 6-31G basis set includes the addition of polarization (d) and diffuse (+) functions on the heavy atoms necessary for a good description of the excited states.[26] As the excited states of these chromophores have charge transfer character, we used the long-range corrected version of B3LYP using the Coulomb-attenuating method.[27] The molecular volume was calculated with the VOLUME=TIGHT keyword. Ground and S_1 state densities and dipole moments were calculated using the DENSITY=ALL keyword.

3. RESULTS AND DISCUSSION

Figure 2 shows the 2PA cross section spectra of the compounds studied (blue symbols). The 1PA spectra (right vertical scale) are shown for comparison. The 2PA spectrum of F shows a feature at λ_{2PA} ~ 750 nm, which most likely belongs to an impurity and will be disregarded in what follows. The fluorescence of NO_2 was too weak (Φ_{fl} < 0.01%), which did not allow reliable evaluation of the σ_2 cross section. In this case, the 2PA spectrum is presented in arbitrary units. We estimate that for the other 10 compounds the experimental uncertainty of the 2PA cross section value is about ±20%.

Both 2PA and 1PA spectra of all 11 compounds display a distinct band that corresponds to the $S_0 \rightarrow S_1$ transition. To find the frequency of the pure electronic (0−0) transition, we fit the two longest wavelength components of the 1PA spectrum with Gaussian curves. The determined in this way peak 0−0 transition frequencies vary from 29 590 cm^{-1} in OCH_3 to 25 510 cm^{-1} in NPh_2 and show good correlation with the calculated 0−0 transition frequencies according to the regression formula:

$$E_{0-0}(\text{expt},\text{cm}^{-1}) = -2883 + 1.006E_{0-0}(\text{calc},\text{cm}^{-1}), \quad r = 0.9863 \tag{1}$$

As the next step, we obtain the peak 2PA cross sections corresponding to the 0−0 transition. This is achieved by applying the same fitting procedure to the 2PA spectrum, where the position and width of the Gaussian functions are fixed from the 1PA spectrum. The resulting 0−0 peak cross sections vary in magnitude from σ_2 = 3.3 GM for *tert*-butyl to σ_2 = 63.0 GM for NPh_2.

In the short wavelength region most compounds show a steep increase of 2PA, starting from about λ_{2PA} ~ 640−660 nm, which may be attributed to the resonance enhancement effect.[13] In addition, the spectra of NPh_2, BT, and NO_2 show a broad band centered at about λ_{2PA} ~ 600 nm. Table 1 summarizes the key 1PA and 2PA properties of the chromophores.

If the 2PA transition between the ground state and an excited electronic state occurs without involving any intermediate states (so-called two-level model), then the maximum 2PA cross section (in GM) may be evaluated from the following relation:[15,16]

$$\sigma_2 = \frac{2(2\pi)^4 f_{opt}{}^4}{15(nch)^2}|\mu|^2|\Delta\mu|^2(2\cos^2\theta + 1)g(2\nu_L) \tag{2}$$

where μ and $\Delta\mu$ are, respectively, the transition dipole moment and the difference of permanent electric dipole moments between the ground state and the excited state, θ is the angle between the two vectors, ν_L is the laser frequency (Hz), f_{opt} is the optical local field factor, n is the refractive index, c is the velocity of light in vacuum, and $g(2\nu_L)$ is the line shape function (Hz^{-1}), normalized according to

$$\int g(x)\,dx = 1 \tag{3}$$

This relation may be also rewritten to express the absolute value of the permanent dipole moment change as a function of the peak 2PA cross section in the same transition:

$$|\Delta\mu| = \left(\frac{5}{4(1+2\cos^2\theta)}\frac{hcN_A}{\pi 10^3 \ln 10}\frac{n}{f_{opt}{}^2}\frac{\nu_{max}}{\varepsilon_{max}}\sigma_2(0-0)\right)^{1/2} \tag{4}$$

dx.doi.org/10.1021/jp200129h |J. Phys. Chem. A XXXX, XXX, 000–000

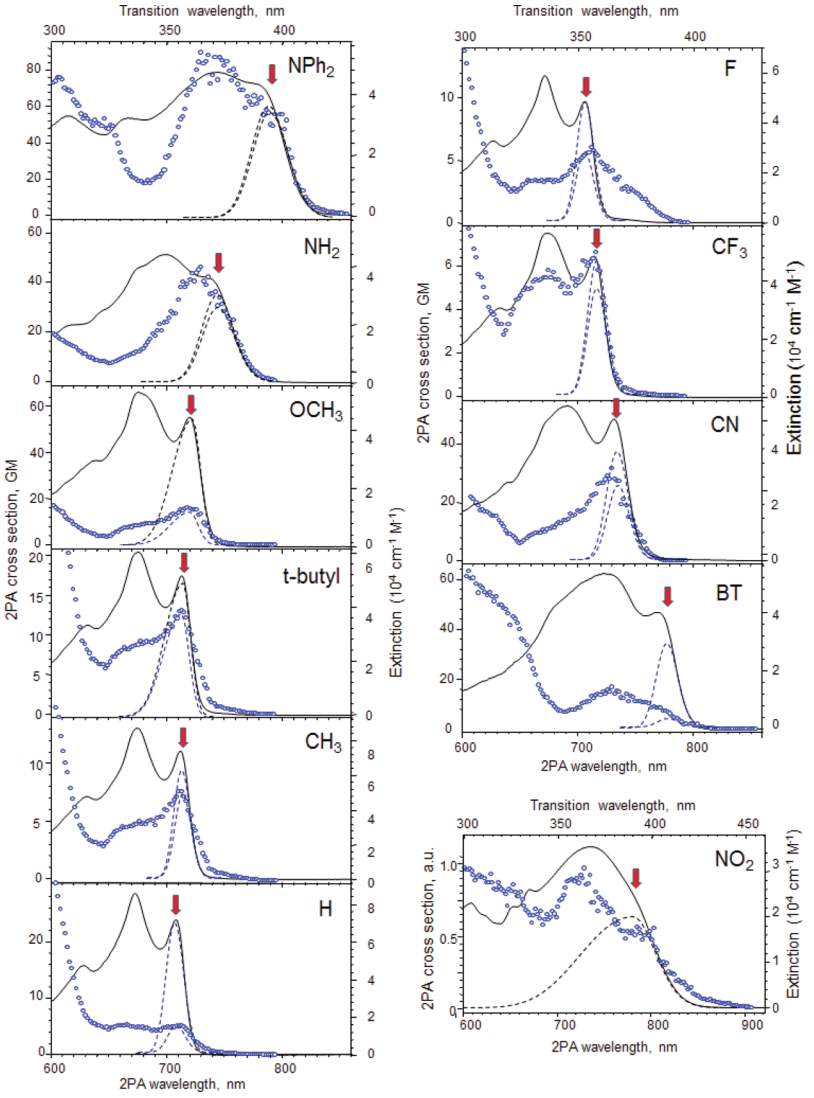

Figure 2. 2PA spectra (blue symbols and left vertical axis) and linear extinction spectra (black solid line and right vertical axis) of the chromophores. Bottom horizontal axis is the 2PA laser wavelength, and the top horizontal axis is the transition (1PA) wavelength.

where $\sigma_2(0-0)$ is the 2PA cross section corresponding to the peak frequency, ν_{max}, of the 0−0 transition, ε_{max} is the corresponding extinction coefficient and N_A is the Avogadro number. In obtaining (4) we take advantage of the relation between $|\mu|^2$ and ε_{max}:[28]

$$|\mu|^2 g(\nu_{max}) = \frac{3 \times 10^3 \ln 10 hc}{(2\pi)^3 N_A} \frac{n}{f_{opt}{}^2} \frac{\varepsilon_{max}}{\nu_{max}} \qquad (5)$$

In elongated or nearly linear-shaped molecules such as those studied here the transition dipole moment vector and the permanent dipole moment vector both tend to align parallel to the long axis of the molecules. Therefore, we may assume that $\theta = 0$. We also assume that the local field factor is, $f_{opt} = (2 + n^2)/3$, with $n = 1.49$ for toluene. Table 1 lists the absolute value of the permanent dipole moment change upon the 0−0 transition found from eq 4. The $|\Delta\mu_{2PA}|$value obtained in this manner turns out to be the largest for NPh_2 (6.8 D) and the smallest for *tert*-butyl (1.4 D).

Next we compare the above experimental results with the quantum chemical calculations. As before, we assume that the transition and permanent dipole moment difference vectors are parallel or nearly parallel, $\theta \approx 0$. Figure 3 shows the correlation between $|\Delta\mu_{calc}|$ and $|\Delta\mu_{2PA}|$. The fact that the calculated and the experimental values agree within ±20% corroborates our above assumptions about the validity of the two-state model as well as the parallel orientation of the dipole moment vectors. Only in the cases of H and F are the experimental values about twice as large as those predicted by the theory. One possible explanation for this deviation is that the two-state model may be less accurate if the cross section is small because the contribution of other excited states acting as intermediate states may have then a comparable value. This deviation may be also caused by an additional dipole moment induced due to the field created in the chromophore by the surrounding solvent molecules, which is not accounted for in the present calculations. Earlier persistent spectral hole-burning Stark effect studies indicate that typical values for the induced dipole moment difference of a molecules in condensed phase could be as large as 0.1−1.0 D.[29] Even larger induced dipole moments have been recently observed in fluorescent protein chromophores.[17]

dx.doi.org/10.1021/jp200129h |*J. Phys. Chem. A* XXXX, XXX, 000–000

Table 1. Summary of One- and Two-Photon Properties of the Compounds Studied[a]

		λ_{abs} (nm) $S_0 \rightarrow S_1$											
R	σ_p	calc	exp	ε_{max} (0−0) (cm^{-1} M^{-1})	τ_{fl} (ns)	Φ_{fl}	$\Delta\nu_{SS}/\Delta f$ (cm^{-1})	a_{calc} (Å)	a_r (Å)	σ_2 (GM)	$\Delta\mu_{calc}$ (D)	$\Delta\mu_{2PA}$ (D)	$\Delta\mu_{SS}$ (D)
NPh_2	−0.22	352	392	40 129	1.28 ± 0.02	0.62	4342	5.36	7.8	63.0	6.8	6.8	11.5
NH_2	−0.66	335	371	26 893	0.98 ± 0.02	0.72	5375	4.99	6.5	18.4	6.0	5.9	11.5
OCH_3	−0.27	328	361	45 021	0.84 ± 0.02	0.86	494	4.91	6.7	16.0	3.4	3.4	3.4
tert-butyl	−0.2	326	357	50 708	0.70 ± 0.02	0.91	237	5.14	7.4	3.3	1.8	1.4	2.5
CH_3	−0.17	325	356	71 971	0.78 ± 0.03	0.95	143	4.90	6.8	7.5	1.7	1.9	1.8
H	0	323	355	71 459	0.77 ± 0.03	1.00	59	4.70	4.9	5.2	0.7	1.8	1.1
F	0.06	323	353	46 514	0.79 ± 0.03	1.00	121	4.74	4.2	5.9	0.8	2.0	1.6
CF_3	0.54	327	357	48 060	1.77 ± 0.02	0.90	599	4.80	7.4	6.4	2.4	2.2	3.6
CN	0.66	335	366	38 972	0.90 ± 0.02	0.75	2010	4.91	6.6	28.9	4.3	4.8	8.8
BT	0.26	354	386	37 343	0.80 ± 0.02	0.69	1014	5.15	8.4	8.1	3.0	2.6	5.2
NO_2	0.78	351	391	20 402		<0.001		4.85			10.0		

[a] σ_p, Hammett constant; λ_{abs}, the calculated (calc) wavelength of the lowest-energy 1PA transition and the measured (exp) wavelength of the 0−0 transition; ε_{max}, the peak extinction coefficient of the 0−0 transition determined by the fitting procedure as described above; τ_{fl}, the fluorescence lifetime; Φ_{fl}, the fluorescence emission quantum yield; $\Delta\nu_{SS}/\Delta f$, the linear slope of the relation between the Stokes shift and the dielectric function of the solvent; a_{calc}, the molecular radius estimated from molecular structure; a_r, the molecular radius estimated from fluorescence anisotropy measurements; σ_2, the peak 2PA cross sections corresponding to the 0−0 transition; $\Delta\mu_{calc}$, the absolute value of the permanent electric dipole moment change in the 0−0 transition determined from quantum mechanical calculations; $\Delta\mu_{2PA}$, the dipole moment determined from the measured 2PA cross section; $\Delta\mu_{SS}$, the dipole moment determined from solvatochromic shift measurements.

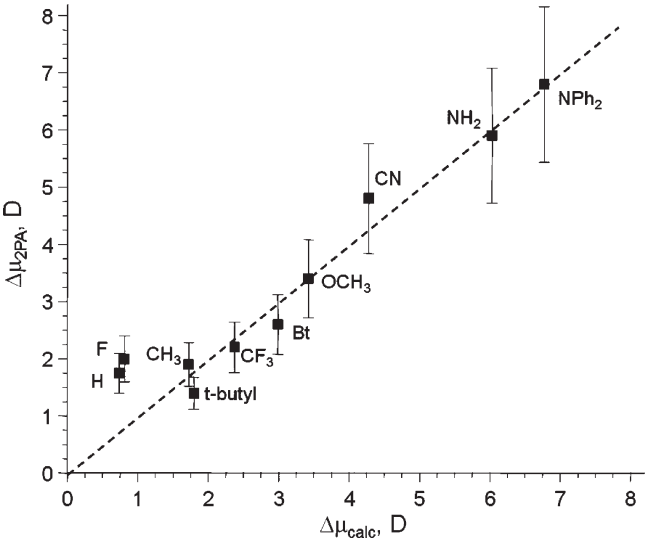

Figure 3. Comparison of the theoretically calculated permanent electric dipole moment difference (horizontal axes) and the values determined from the 2PA cross sections (vertical axes). Estimated experimental error is ±20%. The diagonal line represents exact coincidence between the two values.

To further elucidate the quantitative relation between the 2PA and the dipolar properties, we determine the effective molecular dipole moment difference, $|\Delta\mu_{SS}|$, using the solvatochromic shift method. For this purpose we measure the dependence of the Stokes shift between the absorption and fluorescence 0−0 transition on the solvent polarity function,[22]

$$F(\varepsilon,n) = \frac{2(\varepsilon-1)}{2\varepsilon+1} - \frac{2(n^2-1)}{2n^2+1} \quad (6)$$

where ε is the dielectric constant and n is the index of refraction of the solvent. Figure 4 shows the measured Stokes shifts plotted as a function of F. As expected, the chromophores with larger electron donating-or withdrawing capacity of the end group show large variation of the solvatochromic shifts with varying polarity of the solvent, whereas in H and F this variation is much smaller. The linear slopes and corresponding standard deviations are determined from linear regression and are listed in Table 1.

The fact that all 10 chromophores show a nearly linear increase of the Stokes shift with the increasing value of F confirms that specific interactions between the solute and the solvent are negligible. Under such conditions, the Stokes shift is related to the molecular permanent dipole moment difference by the equation:[30]

$$|\Delta\mu_{ss}|^2 = hca^3\frac{\Delta\bar{\nu}_{ss}}{\Delta F} \quad (7)$$

where $\Delta\bar{\nu}_{SS}/\Delta F$ is the linear slope of the Stokes shift (in cm^{-1}) and a is the radius corresponding to some effective spherical cavity that the molecule occupies inside the dielectric. One way to obtain the radius is from the calculated molecular volume, with the assumption that the effective space occupied by the molecule may be approximated by a sphere ($V_{mol} = 4\pi a^3/3$). As expected, the difference between the largest and the smallest radius values is only about 10%. The radius may be also estimated by measuring the anisotropy of the fluorescence emission.[15] We measured the anisotropy of the $S_1 \rightarrow S_0$ transition for each of the 10 chromophores in a series of solvents with varying viscosity and then estimated the effective molecular radius from the Perrin equation:[22]

$$\frac{r_0}{r} = 1 + \frac{\tau_{fl}k_BT}{\eta V_{mol}} \quad (8)$$

where r is the static anisotropy, r_0 is the limiting anisotropy, η is the viscosity of the solvent, τ_{fl} is the fluorescence decay time, T is the temperature, k_B is the Boltzmann constant, and V_{mol} is the volume of the spherical cavity. The fluorescence decay curves and the Perrin plots are presented in the Supporting Information. Table 1 lists the molecular radius values a_{calc} and a_r obtained by the two alternative methods.

dx.doi.org/10.1021/jp200129h |J. Phys. Chem. A XXXX, XXX, 000–000

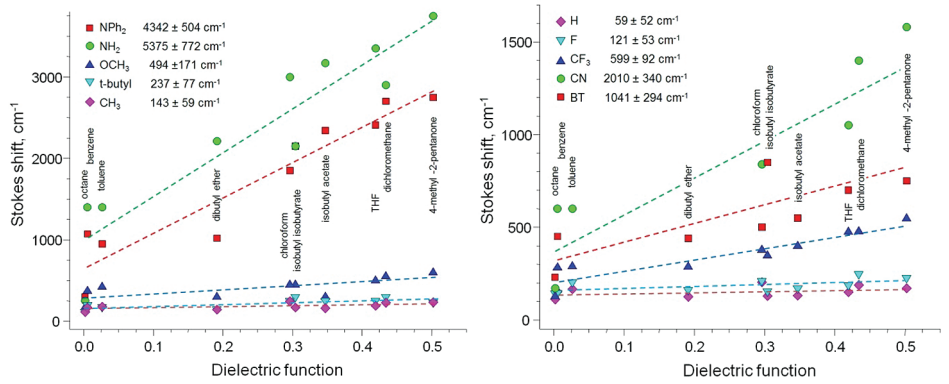

Figure 4. Stokes shift measured in 10 different solvents. Dashed lines represent best linear fits for each chromophore. The inset shows the slope values and the corresponding standard deviation.

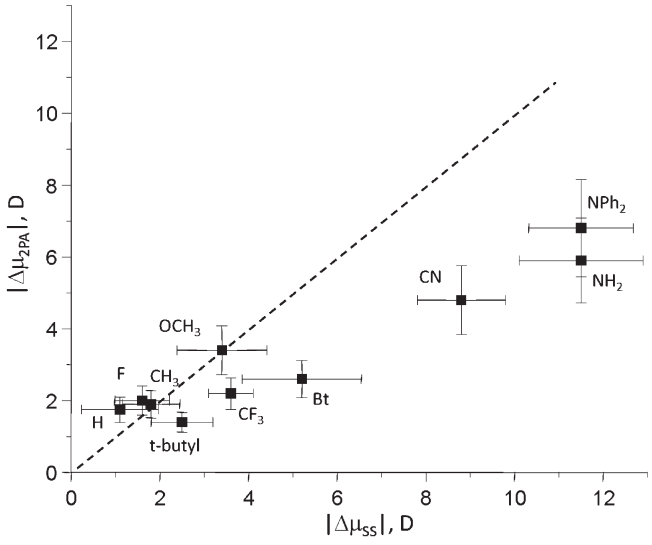

Figure 5. Correlation between the permanent dipole moment difference obtained from solvatochromic shift (horizontal axis) and the values obtained from the 2PA cross section (vertical axis). The diagonal line represents exact coincidence between the two values.

Comparing a_r to a_{calc} reveals that the two values coincide within the error margin for the neutral chromophores such as H and F, while for the chromophores with the strongest electron withdrawing or electron donation end group the value of a_r is up to 80% larger. This discrepancy can be attributed in part to the dependence of the depolarization rate on the nonspherical shape of the molecules, which is neglected in the current simple model.[22] It has been reported that in some cases the depolarization rate may change even when the differences in the shape factors are small.[31] However, the fact that the difference between the two values increases with increasing $\Delta\mu$ suggests that properties other than the nonspherical shape may play a role. For this reason we use a_{calc} to find the corresponding values of $|\Delta\mu_{SS}|$ listed in Table 1.

Figure 5 shows the permanent dipole moments differences obtained from the 2PA cross section with respect to the values obtained from the solvatochromic shift measurements. For the chromophores with small permanent dipole moment difference, such as H, F, CH_3, and OCH_3, the agreement is within the experimental error margins. On the other hand, for the chromophores with larger dipole moments, such as NH_2 and NPh_2, the value obtained from the solvatochromic experiment exceed considerably those determined from 2PA spectra as well as the calculated values. Since the dielectric cavity volume assumed here is already close to the smallest possible, this could mean that for those chromophores with the strongest ED or EW end groups the actual discrepancy may be even larger, up to a factor of 5.

To rationalize these results, we notice that in all the compounds studied here the substitution occurs only at one end of the molecule, while the center and the other end remain unchanged. In the case of strong ED or EW end groups, of those parts that remain constant only those atoms that are closest to the variable end group have an appreciable contribution to the charge transfer, while the rest of the molecule remains essentially neutral. This means that upon the transition from the ground state to the excited state the variation of the charge distribution responsible for the largest $\Delta\mu$ is mostly localized on the substituted end of the molecule. At this point we may recall that 2PA is well described in the point dipole approximation. In other words, the dipole moment difference that is determined from the measurement of the 2PA (e.g., according to eq 4) does not depend on the exact location of the charges within the molecule simply because the optical wavelength is so much larger than the size of the molecule. Solvatochromic shifts, on the other hand, occur as a result of interaction with immediate surroundings of the molecule and thus depend on the location and the distances between the charges. Standard Onsager theory[32] describes solvatochromic shift in terms of a change of the electrostatic energy of a point dipole located at the center of an effective cavity inside a continuous dielectric. If, however, the point dipole is displaced from the center, then the interaction energy increases as the distance from the dipole and the closest cavity wall decreases.[33] If the chromophores with stronger ED and EW property indeed displace the effective point dipole toward one end of the molecule, then this may explain why the $|\Delta\mu|$ values obtained from the solvatochromic shifts are overestimated for the chromophores having the large 2PA cross sections.

4. SUMMARY AND CONCLUSIONS

We use wavelength-tunable femtosecond laser pulses to investigate the 2PA spectra and cross sections in a series of fluorenyl-based chromophores end-capped with 10 different groups with systematically varying electron donating or electron

dx.doi.org/10.1021/jp200129h |J. Phys. Chem. A XXXX, XXX, 000–000

withdrawing strengths and show that the character of the end group influences the 2PA cross section in a systematic manner. By measuring the 2PA in the lowest electronic transition, we show that substituents with the strongest EW or ED character give rise to larger 2PA, up to $\sigma_2 \sim 60$ GM, while neutral substituents provide only a small 2PA cross section, $\sigma_2 < 10$ GM. Following the two-level model, we use the peak value of the 2PA cross section in the 0−0 transition to determine the change of the permanent electric dipole moment in the same transition and achieve good quantitative correlation to the values obtained by quantum chemistry calculations. We then further elucidate the quantitative relation between the 2PA and the change of the permanent dipole moment by carrying out solvatochromic measurements. We show that the permanent dipole moment difference obtained by all three methods correlate well for the chromophores with less strong EW or ED substitutents. However, molecules with stronger ED/EW substituents tend to give larger Stokes shifts, which causes an overestimation of the dipole moment difference. This discrepancy may be attributed to the nonsymmetrical structure of the molecules, where the effective point dipole is shifted off the center toward the substituted end of the molecule. Of course, the above very simple picture may not be fully adequate, especially if we consider that the Lippert formula is based on several approximations not discussed here, not to mention that the accuracy of our solvatochromic shift measurements is low especially when the frequency shifts are accompanied by considerable broadening of the bands. Nevertheless, we believe that this work has shown that 2PA spectroscopy is a valuable tool for determining permanent molecular dipoles, especially under conditions when traditional methods such as solvatochromic shift are not sufficiently accurate or even not applicable. We also believe that these results improve the understanding of the molecular origin of the 2PA properties and may eventually lead to functionalized 2PA chromophores that can be designed for particular applications by means of combining modular groups with known properties.

■ ASSOCIATED CONTENT

Supporting Information. Figure S1 shows the fluorescence decay curves measured in chloroform solution using a C5680-21 synchro-scan streak camera (Hamamatsu). The fluorescence was excited with frequency-doubled output of a mode-locked Ti:sapphire femtosecond oscillator (Coherent Mira 900). The excitation wavelength was tuned to coincide with the linear absorption of the sample. Lifetime values were obtained by fitting the data with a single exponential function. Figure S2 shows the Perrin plots used to determine the effective radius of the chromophores. The fluorescence anisotropy was measured at room temperature in six mixtures of chloroform and castor oil in the following volume proportions: 1:0, 2:1, 3:2, 2:3, 1:4, and 0:1. The viscosity varied between minimum value $\eta = 0.58 \times 10^{-2}$ cm^2 s^{-1} (pure chloroform) and maximum value $\eta = 10.17$ cm^2 s^{-1} (pure castor oil). This material is available free of charge via the Internet at http://pubs.acs.org.

■ AUTHOR INFORMATION

Corresponding Author

*E-mail: A.R., rebane@physics.montana.edu; T.M.C., Thomas.Cooper@wpafb.af.mil.

Present Addresses

[§]Department of Chemistry, Georgia Institute of Technology, Altanta, GA 30332.

■ ACKNOWLEDGMENT

We are thankful for the support of this work by AFRL/RX contract F33615-03-D-5408 for D.M.K. and A.R.B., FA9550-09-1-0219 for A.R., N.S.M., and E.B.

■ REFERENCES

(1) Goepper-Mayer, M. *Ann. Phys.* **1931**, *9* (2), 275–294.
(2) Denk, W.; Strickler, J. H.; Webb, W. W. *Science* **1990**, *248*, 73.
(3) (a) Parthenopoulos, D. A.; Rentzepis, P. M. *Science* **1989**, *245*, 843–845. (b) Makarov, N. S.; Rebane, A.; Drobizhev, M.; Wolleb, H.; Spahni, H. *J. Opt. Soc. Am. B* **2007**, *24* (8), 1874–1885.
(4) Sutherland, R. L.; Brant, M. C.; Heinrichs, J.; Rogers, J. E.; Slagle, J. E.; McLean, D. G.; Fleitz, P. A. *J. Opt. Soc. Am. B* **2005**, *22*, 1939.
(5) Cumpston, B. H.; Ananthavel, S. P.; Barlow, S.; Dyer, D. L.; Ehrlich, J. E.; Erskine, L. L.; Heikal, A. A.; Kuebler, S. M.; Lee, I. Y. S.; McCord-Maughon, D.; Qin, J. Q.; Rockel, H.; Rumi, M.; Wu, X. L.; Marder, S. R.; Perry, J. W. *Nature* **1999**, *398* (6722), 51–54.
(6) Starkey, J. R.; Rebane, A. K.; Drobizhev, M., A.; Meng, F.; Gong, A.; Elliott, A.; McInnerney, K.; Spangler, C. W. *Clin. Cancer Res.* **2008**, *14* (20), 6546–6573.
(7) Pawlicki, M.; Collins, H. A.; Denning, R. G.; Anderson, H. L. *Angew. Chem. Int. Ed.* **2009**, *48*, 3244–3266.
(8) Terenziani, F.; Katan, C.; Badaeva, E.; Tretiak, S.; Blanchard-Desce, M. *Adv. Mater.* **2008**, *20* (24), 4641–5678.
(9) He, G. S.; Tan, L. S.; Zheng, Q.; Prasad, P. N. *Chem. Rev.* **2008**, *108* (4), 1245–1330.
(10) Spangler, C. W. *J. Mater. Chem.* **1999**, *9* (4), 2013–2020.
(11) Boyd, R. *Nonlinear Optics*, 3rd ed.; Academic Press: New York, 2008.
(12) Albota, M.; Beljonne, D.; Bredas, J.-L.; Ehrlich, J. E.; Fu, J.-Y.; Heikal, A. A.; Hess, S. E.; Kogej, T.; Levin, M. D.; Marder, S. R.; McCord-Maughon, E.; Perry, J. W.; Rockel, H.; Rumi, M.; Subramaniam, G.; Webb, W. W.; Wu, X.-L.; Xu, C. *Science* **1998**, *281*, 1653.
(13) Drobizhev, M.; Karotki, A.; Kruk, M.; Rebane, A. *Chem. Phys. Lett.* **2002**, *355* (1−2), 175–182.
(14) (a) Callis, P. R.; Scott, T. W.; Albrecht, A. C. *J. Chem. Phys.* **1981**, *75* (12), 5640–5646. (b) Dick, B.; Hohleneicher, G. *J. Chem. Phys.* **1982**, *76* (12), 5755–5760. (c) Birge, R. R.; Zhang, C.-F. *J. Chem. Phys.* **1990**, *92*, 7178–7180.
(15) Rebane, A.; Makarov, N. S.; Drobizhev, M.; Spangler, B.; Tarter, E. S.; Reeves, B. D.; Spangler, C. W.; Meng, F. Q.; Suo, Z. Y. *J. Phys. Chem. C* **2008**, *112* (21), 7997–8004.
(16) (a) Drobizhev, M.; Meng, F. Q.; Rebane, A.; Stepanenko, Y.; Nickel, E.; Spangler, C. W. *J. Phys. Chem. B* **2006**, *110* (20), 9802–9814. (b) Drobizhev, M.; Makarov, N. S.; Rebane, A.; de la Torre, G.; Torres, T. *J. Phys. Chem. C* **2008**, *112* (3), 848–859. (c) Rebane, A.; Drobizhev, M. A.; Makarov, N. S.; Beuerman, E.; Nacke, C.; Pahapill, J. *J. Lumin.* **2010**, *130* (6), 1055–1059.
(17) Drobizhev, M.; Tillo, S.; Makarov, N. S.; Hughes, T. E.; Rebane, A. *J. Phys. Chem. B* **2009**, *113* (39), 12860–12864.
(18) Rogers, J. E.; Slagle, J. E.; Krein, D. M.; Burke, A. R.; Hall, B. C.; Fratini, A.; McLean, D. G.; Fleitz, P. A.; Cooper, T. M.; Drobizhev, M.; Makarov, N. S.; Rebane, A.; Kim, K.-Y.; Farley, R.; Schanze, K. S. *Inorg. Chem.* **2007**, *46*, 6483.
(19) Drobizhev, M.; Karotki, A.; Dzenis, Y.; Rebane, A.; Suo, Z. Spangler, C. W. *J. Phys. Chem. B* **2003**, *107* (31), 7540–7543. Drobizhev, M.; Rebane, A.; Suo, Z.; Spangler, C. W. *J. Lumin.* **2005**, *111* (4), 291–305.
(20) Haley, J. E.; Krein, D. M.; Monahan, J. L.; Burke, A. R.; McLean, D. G.; Slagle, E.; Fratini, A.; Cooper, T. M. *J. Phys. Chem. A* **2010**in press.
(21) Lakowicz, J. R. *Principles of Fluorescence Spectroscopy*, 3rd ed.; Springer: Berlin, 2006.

(22) *Handbook of Chemistry and Physics*, 83rd ed.; CRC Press: Boca Raton, FL, 2002.
(23) Demas, J. N.; Crosby, G. A. *J. Phys. Chem.* **1971**, *75*, 991.
(24) Makarov, N. S.; Drobizhev, M.; Rebane, A. *Opt. Express* **2008**, *16* (6), 4029–4047.
(25) Frisch, M. J.; Trucks, G. W.; Schlegel, H. B.; Scuseria, G. E.; Robb, M. A.; Cheeseman, J. R.; Scalmani, G.; Barone, V.; Mennucci, B.; Petersson, G. A.; Nakatsuji, H.; Caricato, M.; Li, X.; Hratchian, H. P.; Izmaylov, A. F.; Bloino, J.; Zheng, G.; Sonnenberg, J. L.; Hada, M.; Ehara, M.; Toyota, K.; Fukuda, R.; Hasegawa, J.; Ishida, M.; Nakajima, T.; Honda, Y.; Kitao, O.; Nakai, H.; Vreven, T.; Montgomery, J. A., Jr.; Peralta, J. E.; Ogliaro, F.; Bearpark, M.; Heyd, J. J.; Brothers, E.; Kudin, K. N.; Staroverov, V. N.; Kobayashi, R. Normand, J.; Raghavachari, K.; Rendell, A.; Burant, J. C.; Iyengar, S. S.; Tomasi, J.; Cossi, M.; Rega, N.; Millam, J. M.; Klene, M.; Knox, J. E.; Cross, J. B.; Bakken, V.; Adamo, C.; Jaramillo, Gomperts, R.; Stratmann, R. E.; Yazyev, O.; Austin, A. J.; Cammi, R.; Pomelli, C.; Ochterski, J. W.; Martin, R. L.; Morokuma, K.; Zakrzewski, V. G.; Voth, G. A.; Salvador, P.; Dannenberg, J. J.; Dapprich, S.; Daniels, A. D.; Farkas, O.; Foresman, J. B.; Ortiz, J. V.; Cioslowski, J. Fox, D. J. *Gaussian 09*, Revision A.02; Gaussian, Inc.: Wallingford, CT, 2009.
(26) Foresman, J. B.; Frisch, A. *Exploring Chemistry with Electronic Structure Methods*, 2nd ed.; Gaussian Inc.: Pittsburgh, 1996
(27) Yanai, T.; Tew, D.; Handy, N. *Chem. Phys. Lett.* **2004**, *393*, 51.
(28) Toptygin, D. *J. Fluoresc.* **2003**, *13* (3), 201–219.
(29) Rebane, A.; Drobizhev, M.; Makarov, N. S.; Beuerman, E.; Hughes, T. E.; Tillo, S. *J. Lumin.* **2010**, *27* (1), 1619–1623.
(30) Suppan, P. *J. Photochem. Photobiol. A Chem.* **1990**, *50* (3), 293–330.
(31) Dutt, G. B.; Ghanty, T. K. *J. Chem. Phys.* **2004**, *121* (8), 3625–3631.
(32) Onsager, L. *J. Am. Chem. Soc.* **1936**, *58*, 1486–1493.
(33) (a) Lindell, I. V. *Radio Sci.* **1992**, *27* (1), 1–8. (b) Norris, W. T. *IEE Proc. Sci. Meas. Technol* **1995**, *142* (2), 142–150.